

Replicating Aneurysm Rupture

Report 2

Anna Mellin: Team, Design, and 3D Printing Lead
Amanda Ortiz-Velazquez: Budget and Testing Lead
Caden Adams: Casting and CAD Lead

Fall 2024-Spring 2025



Project Sponsor: Dr. Zhongwang Dou
Instructor: Dr. David Willy

DISCLAIMER

This report was prepared by students as part of a university course requirement. While considerable effort has been put into the project, it is not the work of licensed engineers and has not undergone the extensive verification that is common in the profession. The information, data, conclusions, and content of this report should not be relied on or utilized without thorough, independent testing and verification. University faculty members may have been associated with this project as advisors, sponsors, or course instructors, but as such they are not responsible for the accuracy of results or conclusions.

EXECUTIVE SUMMARY

Cerebral aneurysms cause approximately 500,000 deaths each year. To address this urgent issue, Dr. Zhongwang Dou, the team's client, has tasked the team with developing a way to create predictable aneurysm rupture models. These models could play a crucial role in preventing and repairing aneurysms. In the final design, the aneurysm model will be suspended in gelatin that simulates the pressure of brain tissue. This model will be connected to a pump that will send a blood-like fluid through the model. Flow and sensor pressures will be placed throughout the system for data collection. The client requires that the models be functional, predictable, and measurable.

The first step of the project was material analysis. A list of criteria that the material must fulfill was created and heat resistance was identified as the most important factor. The material's ability to maintain shape, even with extremely thin walls, was also considered a key component. These specifications resulted in the decision to use methods using 3D-printed material and silicone. The next step was to develop hollow models and molds within SolidWorks. Constructing the hollow models proved to be simpler than designing the molds. A three-part mold was one of the methods chosen to develop the hollow model. This consisted of a solid version of the aneurysm that would fit into the cavity of a two-part shell. The solid models required supports to ensure stability and contain the silicone within the mold. The cavity itself would be in the shape of the aneurysm geometry with a space of 0.75 mm to maintain even silicone distribution along the walls. The team experimented with different mold designs, which included versions with holes and keys. The final design, however, had neither.

Once the design was finalized, the resin printer and Idea Lab were used to produce the physical models. Both the Idea Lab prints and the resin printer using ABS-like material posed several issues. However, after several failed iterations, the team successfully created the full three-part mold and the hollowed model for the idealized aneurysm. In the upcoming weeks, different methods of filling the three-part mold with silicone will be tested and refined before then printing the core with water-soluble material. Dissolving the water-soluble core to create a hollow model will be the final step in preparing the product for testing.

Though similar aneurysm rupture simulations exist, this project aims to focus on quick, cost-effective production. The \$1,000 budget will fund the manufacturing process and the various tests that will be conducted to understand how effectively the model simulates aneurysm behavior, and the rupture of the aneurysm itself. The client emphasized the necessity of easy replication in this project, which means that creating the most economic parts and methods is crucial to success.

Once the idealized model simulation is repeatable and predictable, the next step is to produce patient-specific models. Having a working model could help advance medical devices and treatments used for aneurysms. This could ultimately help prevent deaths caused by aneurysm ruptures.

Contents

DISCLAIMER.....	1
EXECUTIVE SUMMARY	2
1 BACKGROUND.....	3
1.1 Project Description.....	4
1.2 Deliverables.....	4
1.3 Success Metrics.....	4
2 REQUIREMENTS.....	5
2.1 Customer Requirements.....	5
2.2 Engineering Requirements.....	5
2.3 House of Quality (HoQ).....	6
3 Research Within Your Design Space.....	7
3.1 Benchmarking.....	7
3.2 Literature Review.....	9
3.2.1 Anna Mellin.....	9
3.2.2 Caden Adams.....	11
3.2.3 Amanda Ortiz-Velazquez.....	13
3.3 Mathematical Modeling.....	15
3.3.1 Velocity Flow Distribution in Ansys CFX - Caden.....	15
3.3.2 Flow Characterization - Anna Mellin.....	17
3.3.3 Estimating Time for Resin to Dissolve - Amanda Ortiz-Velazquez.....	18
4 Design Concepts.....	19
4.1 Functional and Physical Decomposition.....	19
4.2 Concept Generation.....	20
4.2.1 Support System.....	20
4.2.2 Negative Molds.....	22
4.2.3 Negative Mold Conception.....	22
4.3 Selection Criteria.....	23
4.4 Concept Selection.....	24
5 Schedule and Budget.....	25
5.1 Schedule.....	25
5.2 Budget.....	26
5.3 Bill of Materials.....	26
6 Design Validation and Initial Prototype.....	27
6.1 Failure Modes and Effects Analysis (FMEA).....	27
6.2 Initial Prototype.....	28
6.3 Additional Engineering Calculations.....	29
6.4 Future Testing Potential.....	30
7 CONCLUSIONS.....	31
8 REFERENCES.....	33
9 Appendix A: Full Gantt Chart.....	1

1 BACKGROUND

This chapter highlights the general goals and direction of the aneurysm rupture modeling project. Two models will be created: idealized and patient-specific, which will be manufactured with the lost-wax

casting method and high-resolution 3D printing. The project seeks to develop a realistic model within a budget of \$1000 and a fundraised \$100. With a functional model, teaching aneurysm anatomy and personalized treatment strategies may become more accessible to low-resource settings.

1.1 Project Description

This project focuses on the development of an aneurysm rupture model. The main objective of this project is to manufacture a model that mimics real-life rupture phenomena. The fluid flows will be measured with pressure sensors and a high-speed camera in order to verify the accuracy of the model. The end goal is to be able to create a model with high repeatability and a predictable burst. Manufacturing methods will consist of the lost-wax casting method and high-resolution 3D printing. These approaches were specified by the client as a means of cheap manufacturing. Our budget is \$1000, with the goal of fundraising 10% or \$100. If the model is both cheap and easy to remanufacture, it becomes more accessible to hospitals and clinics with smaller budgets. Not only would this create a perfect mechanism for teaching aneurysm anatomy and function in underprivileged areas, but patient-specific aneurysms may be quickly replicated, allowing for doctors to examine the aneurysm more thoroughly and determine the best treatment approach.

1.2 Deliverables

The major deliverables for this project are provided by our client Dr. Zhongwang Dou. The expected yields of this project are an idealized aneurysm model and a patient-specific model. The idealized model consists of a small sphere with two cylindrical legs that stick out at roughly a 120-degree angle. The patient-specific model is derived from a model given by Dr. Dou's laboratory. The lost-wax casting method and high-resolution 3D printing will be utilized to develop cheap and accurate models. The final models will be constructed of elastic silicone and must be easily tested with pressure sensors and a high-speed camera attached to a pump configuration. This pump setup will replicate the human cardiovascular system pumping blood into the aneurysm. The final deliverable is to make the aneurysm rupture.

1.3 Success Metrics

The project will be noted as a success when both idealized and patient-specific models are manufactured quickly and accurately. A current production timeframe is not set but will be defined once a working model is created. Once a working model has been produced, it must also be connectable to the pump configuration and accurately depict aneurysm blood flow. The aneurysm must be able to rupture, and the final metric of success will be forcing the rupture to occur within a minute.

To be more specific, the aneurysm walls must emulate the characteristics of human vessel walls. The current benchmarks prioritize geometry over behavior, which leads to less accurate simulations. This will be tested by comparing current data of blood flow and vessel wall behavior to that of the models. By using the high-speed camera setup, the flow can be analyzed. Additionally, wall characteristics may be assessed using a rheometer to understand the elastic silicone shear stress and strain threshold compared to a vessel wall. Equations such as Laplace's Law, Poiseuille's Flow, Navier-Stokes, and the equation for arterial pressure—all explained further in a later section—will help with calculating the forces within the aneurysm and provide a prediction for when the aneurysm wall will fail. The Noyes-Whitney equation will allow the prediction of manufacturing times and assist in determining the most efficient means of production.

2 REQUIREMENTS

This chapter outlines the engineering and customer-specific requirements laid out for this project with the end goal of creating a cost-effective and easily reproducible aneurysm rupture model. The engineering requirements focus on parameters such as material strength, accurate simulation of aneurysm behavior ease of construction, and repeatability of vessel geometries. These criteria ensure that the aneurysm can produce consistent results. On the customer side, the primary needs include ease of use, affordability, and a different predictable geometry for patient-specific and idealized models. Meeting these requirements is critical to creating a substantial product capable of predicting aneurysm ruptures within 60 seconds of starting fluid flow.

2.1 Customer Requirements

The customer requirements for this project are low cost, predictability of rupture, patient-specific and idealized rupture models, and low labor requirements. The customer laid this out in the first debrief, in which a budget of \$1000 was established. The requirement for rupture predictability stems from the project's need for data collection through an inlet and outlet, transparent vessels, and the targeted application of chemicals to create a thin wall in the aneurysm. This allows the direct observation of ruptures and deformations. Patient-specific and idealized models are required to give a broader testing basis than perfect geometry vessels every time. The patient-specific models are taken from the Vascular Model Repository [2] and when testing commences, the goal is to analyze at least 4 different patient-specific geometries. The low labor requirement ensures that rapid turnaround on new geometries is economically feasible and considers that each model can endure one test before rupture, so new model creation is imperative for a strong testing background.

2.2 Engineering Requirements

The engineering requirements for this project are dimensional accuracy of models, repeatability of tests through model consistency, provision of both a wax cast and 3D printed soft material model for all specified geometries, material cost and availability, and ease of construction. Dimensional accuracy requires the wall thicknesses to be within 0.15 mm of real observed aneurysms of large model geometries. Model consistency stems from the fact that the team needs accurate testing parameters, which begin with the model being tested. Providing both a wax cast and 3D printed model for all geometries creates a wider scope of potential methods moving forward and comparable results between two materials of the same dimensions, the goal for this requirement is recording an error of <2% between tests of the same model, and an error of less than <10% for tests comparing different models. Cost stems from the fact that most of the printing work done in this project is done with resin, primarily water-soluble resin, which is incredibly costly but required for the desired accuracy of the prints. The target is to have each iteration of the project cost less than \$50. Finally, ease of manufacturing is an important requirement as a rapid print turnaround on vessels will be necessary once testing begins. The target for this requirement is a construction time of under 1 hour to get the full system operating. This is excluding printing time and other idle time.

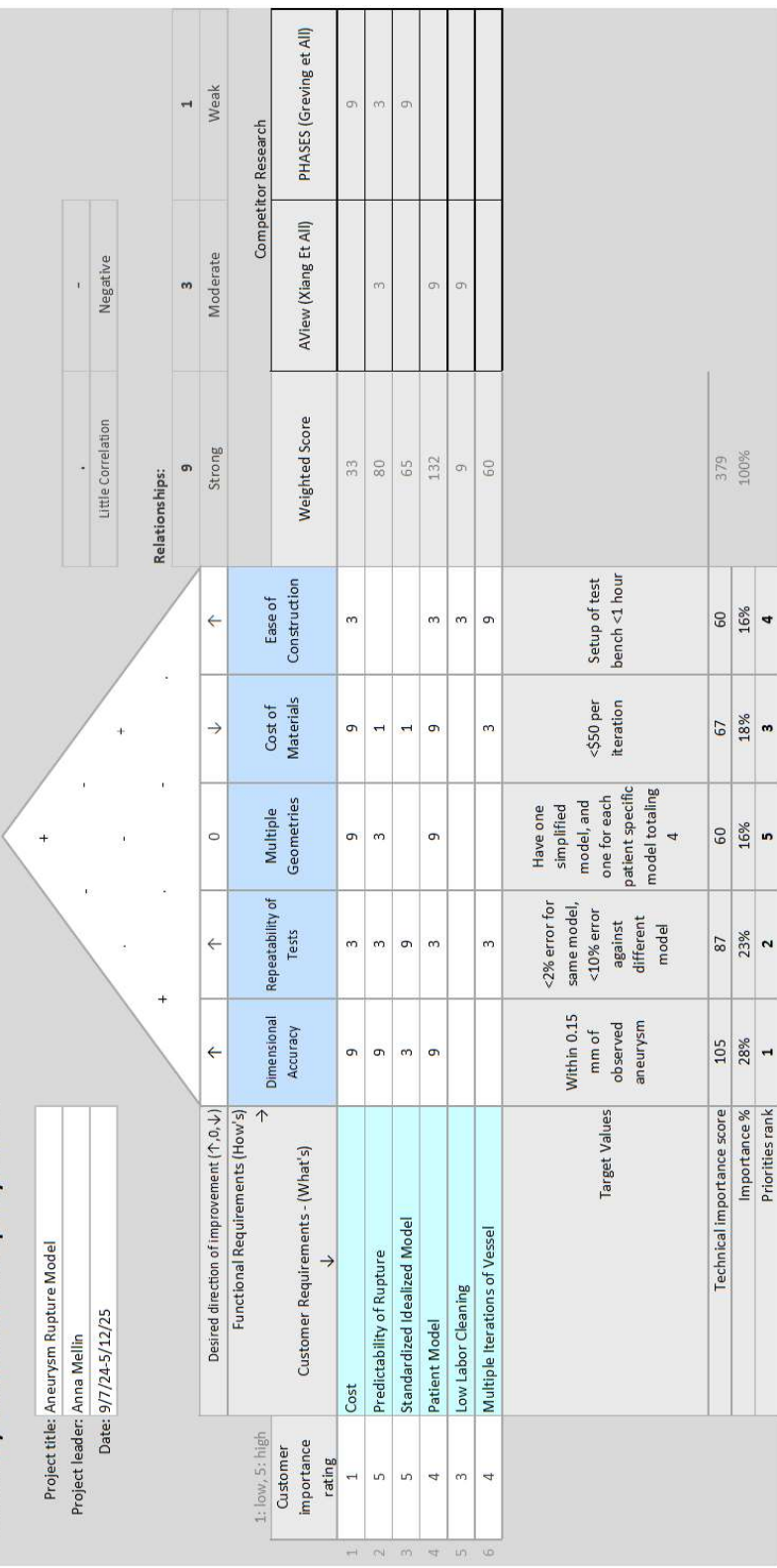
2.3 House of Quality (HoQ)

Quality Function Deployment

Project title: Aneurysm Rupture Model

Project leader: Anna Mellin

Date: 9/7/24-5/12/25



3 Research Within Your Design Space

3.1 Benchmarking

Benchmarking is used to compare current designs to the ones in progress. The point is to take into account existing products and either find the faults that can be improved or use the strengths to incorporate them into the new design. The benchmark characteristics targeted for analysis were working models of aneurysms based on patient-specific geometry. Because the goal of this project is to create a replica of a cerebral aneurysm and test it with a fluid flow system, the best standards must also do the same. This section looks at the mode of production, cost, and general effectiveness. The first benchmark was the Kono Aneurysm shown in Figure 1 [5].



Figure 1 : Kono Aneurysm Model

A 3D-printed vessel and aneurysm model is laid in a silicone block to create the desired geometry which is later dissolved to form the aneurysm-shaped cavity in the block. The process of development and testing took roughly two weeks to complete and cost a total of \$600. The actual creation timeframe is not given. One of the main issues with this model is that the walls of the aneurysm were much stiffer than those of an actual vessel wall. By not following the behavior of a real aneurysm, the ability to use this to simulate treatment is limited.

The capstone model is currently estimated to require two days for development: a day for printing and curing the molds, and a day for allowing the silicone to cure. Assuming numerous models of the same geometry are to be made, only the water-soluble core needs to be printed numerous times. Additionally, with less silicone, the curing time of the capstone model would be significantly lower than that of the Kono Model.

The second chosen benchmark was the Sugiu Model which is comprised of two parts, a rigid model, like the Kono Model situated in a block of silicone, and a soft model which only consists of the model walls, rather than floating in silicone (Figure 2) [6].

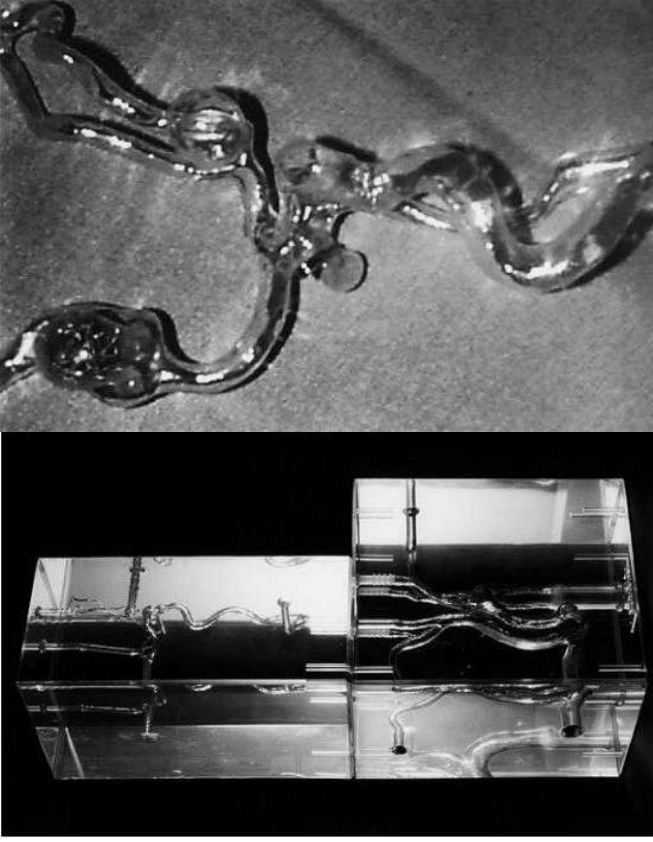


Figure 2: Sigui Models: rigid model (left) and soft model (right)

The rigid model faced the same issues as the Kono Model, but the soft is closer to the objective of the capstone model. The main difference between the soft model and the capstone model is the method of production. The soft model was created via a lost-wax method and the silicone was applied by brushing on layers. This can lead to uneven wall thickness and striations left from the brush. The capstone model, with a uniform gap between the negative and positive molds, forces a uniform wall thickness, assuming the silicone is distributed without air bubbles. The capstone model is projected to require less labor and less attention to detail, making the model easier to manufacture and more geometrically accurate than the soft Sigui Model.

The final benchmark chosen is the Liu Model, which is seemingly the most similar to the current capstone objectives [7]. Numerous models were made including a ruptured vessel, a collapsed vessel, a regular vessel, an uneven vessel, and a rigid vessel (Figure 3).



Figure 3: Liu Model- ruptured vessel, a collapsed vessel, a regular vessel, an uneven vessel, and a rigid vessel, respectively

The Liu Model is very cheap at under \$25 per model. The method of creation is similar to the soft Sigui Model and uses a coating technique rather than a three-part mold. Additionally, the methods for constructing the blister bulges shown in Figure 4 may be duplicated in the capstone model to examine different methods in reproducing aneurysms. The Liu Model uses both hard and soft silicone to allow the blister bulge to form, but it may also cause the vessel wall properties to stray from real-life characteristics.

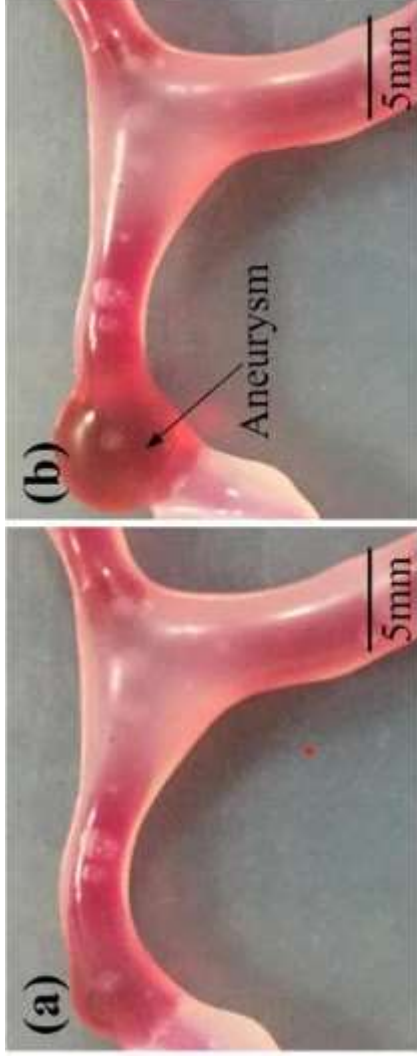


Figure 4: Blister bulge in Liu Model

These benchmarks construct a price range to aim for, as well as provide certain capabilities of aneurysm models currently on the market. By using a different technique than those already formulated, an easier, cheaper, and faster model may be developed to advance the medical field.

3.2 Literature Review

3.2.1 Anna Mellin

[2] “Vascular Model Repository,” *Vascularmodel.com*, 2024. <https://www.vascularmodel.com/index.html> (accessed Sep. 14, 2024).

This archive contains scans of real patient cardiovascular systems which can be used in further development of patient specific cerebral aneurysm models.

[3] R. Fox, A. McDonald, and J. Mitchell, *Fox and McDonald's Introduction to Fluid Mechanics*, 10th ed. 111 River Street Hoboken, NJ: John Wiley & Sons, 2020.

This textbook is a reliable source of how fluid dynamics work which will be important for observing the behavior of fake blood flow within the capstone model.

[4] Mayo Clinic, “Brain aneurysm - Symptoms and causes,” *Mayo Clinic*, Mar. 07, 2023. <https://www.mayoclinic.org/diseases-conditions/brain-aneurysm/symptoms-causes/syc-20361483>

This medical website briefly defines a brain aneurysm and provides background information specifically useful for non-medical professionals.

[5] Kono K, Shintani A, Okada H, Terada T. Preoperative simulations of endovascular treatment for a cerebral aneurysm using a patient-specific vascular silicone model. *Neurol Med Chir (Tokyo)*. 2013;53(5):347-51. doi: 10.2176/nmc.53.347. PMID: 23708228.

A silicone model of an unruptured brain aneurysm is used to simulate treatment plans such as balloon-assisted coil embolization. The model was based on a 3D image of a patient's aneurysm, 3D printed with acrylate photopolymer (light-activated resin) using the Vision Realizer RVS-G1. This model was then set in a block of silicone. When cured, the acrylate photopolymer was removed, leaving a cast of the aneurysm behind. This resulted in an easier application of

treatment, with a significant difference noted: the real-life vessel was much more sensitive to catheter applications, causing slight differences between the simulation and the actual treatment. The main difference between this project and the capstone project is that the Kono Model only takes geometry into account rather than emulating the properties and reactions of the aneurysm.

[6] Sugiu K, Martin JB, Jean B, Gailloud P, Mandai S, Rufenacht DA. Artificial cerebral aneurysm model for medical testing, training, and research. *Neurol Med Chir (Tokyo)*. 2003 Feb;43(2):69-72; discussion 73. doi: 10.2176/nmc.43.69. PMID: 12627882.

Two models were created using the 'lost wax' technique, one hard and one soft. The hard model was created out of a solid silicone block where the aneurysm structure was melted out leaving behind the impression of the aneurysm. The soft model was made via painting 4-6 layers of silicone on the wax model and then melting the wax leaving behind the phantom model that replicated the properties of the vessel walls better.

[7] Liu, Y. *et al.* Fabrication of cerebral aneurysm simulator with a desktop 3D printer. *Sci. Rep.* 7, 44301; doi: 10.1038/srep44301 (2017).

Numerous models were made using the same techniques. The main process included 3D printing a core with PVA and using a coating technique to cover the model in silicone. Both hard and soft silicones were used in order to replicate a bulge to simulate aneurysm formation. The PVA was then dissolved leaving behind a hollow model perfect for flow analysis.

[8] J. R. Ryan, K. K. Almefty, P. Nakaji, and D. H. Frakes, "Cerebral Aneurysm Clipping Surgery Simulation Using Patient-Specific 3D Printing and Silicone Casting," *World Neurosurgery*, vol. 88, pp. 175–181, Apr. 2016, doi: <https://doi.org/10.1016/j.wneu.2015.12.102>.

Not discussed in the main three benchmarks as a more accurate model was found. An anatomically correct model was created via 3D printing using photopolymer (Objet500 Connex multimaterial printer) and 2-part silicone casting (used for the skull). This was developed to assist medical students in becoming familiar with cerebral anatomy and aneurysm clipping. A skull model was created to incorporate the brain aneurysm to familiarize the medical students with a non-isolated aneurysm. Although used for aneurysm clipping procedural practice, to the best of the team's understanding, there is no mention of simulating the aneurysm properties (although the skull is meant to replicate its respective properties) but rather this method is focused on helping students with anatomy identification. This may help the capstone model in correcting patient specific geometry.

[9] N. Hopkinson, Richard Hague, and Philip Dickens, *Rapid Manufacturing An Industrial Revolution for the Digital Age*. The Atrium, Southern Gate, Chichester, West Sussex PO19 8SQ England: John Wiley & Sons, Ltd, 2006.

This book is a great source for understanding additive manufacturing and standards.

[10] "Flow Diversion with Stents for Brain Aneurysms," Dec. 28, 2022, <https://www.hopkinsmedicine.org/health/treatment-tests-and-therapies/flow-diversion-with-stents-for-brain-aneurysms#:~:text=What%20is%20flow%20diversion%20for>

This website illustrates flow diversion with a stent treatment plan for brain aneurysms. Brain stents are a common form of treatment for cerebral aneurysms.

[11] “Endovascular Coiling,” *John Hopkins Medicine*, 2019. <https://www.hopkinsmedicine.org/health/treatment-tests-and-therapies/endovascular-coiling>

This website describes another treatment plan involving coils of platinum metal being inserted into the aneurysm to promote clotting and take pressure off the weakened wall.

[12] “Microsurgical Clipping and Endovascular Coiling for Brain Aneurysm,” www.hopkinsmedicine.org. <https://www.hopkinsmedicine.org/health/treatment-tests-and-therapies/microsurgical-clipping-and-endovascular-coiling-for-brain-aneurysm>

This website provides information about clipping as a means of treatment for brain aneurysms.

3.2.2 Caden Adams

[13] R. G. Nagassa, P. G. McMenamin, J. W. Adams, M. R. Quayle, and J. V. Rosenfeld, “Advanced 3D printed model of middle cerebral artery aneurysms for neurosurgery simulation,” *3D Printing in Medicine*, vol. 5, no. 1, Aug. 2019, doi: <https://doi.org/10.1186/s41205-019-0048-9>.

This article depicts a simple wax-casting method to create a vascular model with a defined aneurysm neck. The process entails the creation of a 3D print of a CAD aneurysm model which is then cast in wax, and painted in several layers of silicone, allowing the wax to be melted through evacuation points leaving a hollow silicone model. This approach allows for a realistic simulation of neurosurgical procedures.

[14] M. S. Pravdivtseva *et al.*, “3D-printed, patient-specific intracranial aneurysm models: From clinical data to flow experiments with endovascular devices,” *Medical Physics*, vol. 48, no. 4, pp. 1469–1484, Feb. 2021, doi: <https://doi.org/10.1002/mp.14714>.

This study delves into the creation of 3D-printed models of intracranial aneurysms specific to patients' aneurysm geometries. The models can be produced within 15-30 hours, allowing for a relatively quick risk analysis and optimal cure procedure.

[15] J. R. Cebal *et al.*, “Aneurysm Rupture Following Treatment with Flow-Diverting Stents: Computational Hemodynamics Analysis of Treatment,” *American Journal of Neuroradiology*, vol. 32, no. 1, pp. 27–33, Nov. 2010, doi: <https://doi.org/10.3174/ajnr.a2398>.

This research investigates the velocity and pressure changes in aneurysms following the implementation of flow-diverting stents using computational fluid dynamics. The use of CFD software is helpful for identifying factors that can lead to both reduced and increased flow rates.

[16] L.-D. Jou and M. E. Mawad, “Analysis of Intra-Aneurysmal Flow for Cerebral Aneurysms with Cerebral Angiography,” *American Journal of Neuroradiology*, vol. 33, no. 9, pp. 1679–1684, May 2012, doi: <https://doi.org/10.3174/ajnr.a3057>.

This article looks at aneurysmal flow using contrast injection. This method allows for non-invasive blood flow analysis through the observation of luminescent particles on the micron level in the blood stream.

[17] W. C. Merritt, H. F. Berns, A. F. Ducruet, and T. A. Becker, “Definitions of intracranial aneurysm size and morphology: A call for standardization,” *Surgical Neurology International*, vol. 12, p. 506, Oct. 2021, doi: https://doi.org/10.25259/SNI_576_2021.

This article goes over the definitions of intracranial aneurysm size. The authors advocate for the standardization of measurements and suggest that wide-neck aneurysms should be the norm for further study.

[18] K. W. Yong, M. Janmaleki, M. Pachenari, A. P. Mitha, A. Sanati-Nezhad, and A. Sen, “Engineering a 3D human intracranial aneurysm model using liquid-assisted injection molding and tuned hydrogels,” *Acta Biomaterialia*, vol. 136, pp. 266–278, Dec. 2021, doi: <https://doi.org/10.1016/j.actbio.2021.09.022>.

This article shines light on a method for engineering 3D intracranial aneurysm models using liquid- injection molding and specialized hydrogels. The process allows for the creation of models that resemble the properties of human tissue, opening the door to a more realistic simulation environment.

[19] C. Patel, “Acquiring Data from Sensors and Instruments Using MATLAB.” Available: <https://www.mathworks.com/content/dam/mathworks/mathworks-dot-com/solutions/automotive/files/in-expo-2012/acquiring-data-from-sensors-and-instruments-using-matlab.pdf>

This document along with the MathWorks website gives readers a guide on using MATLAB for gathering data from sensors and instruments. It covers the fundamental methods for connecting and collecting data, which gives the team a good option for when flow sensors are added into the testing phase.

[20] L. Bousset *et al.*, “Aneurysm Growth Occurs at Region of Low Wall Shear Stress,” *Stroke*, vol. 39, no. 11, pp. 2997–3002, Nov. 2008, doi: <https://doi.org/10.1161/strokeaha.108.521617>.

This study looks at the relationship between wall shear stress and aneurysm growth, finding that regions of low shear stress are more likely to expand and rupture. The findings suggest that wall shear stress may be a strong factor in predicting aneurysm risk.

[21] The Engineering Toolbox, “Dynamic Viscosity of common Liquids,” *Engineeringtoolbox.com*, 2019. https://www.engineeringtoolbox.com/absolute-viscosity-liquids-d_1259.html

This online resource provides a comprehensive list of dynamic viscosity values for various liquids, used primarily for hemodynamic analysis in this project.

[22] F. M. White, *Fluid Mechanics*, 7th ed. McGraw Hill, 2011.

This textbook was used in the team’s fluid dynamics class, offering a wealth of fluid mechanics principles. It is a valuable resource for understanding the fluid mechanics taking place in this project, in a digestible setting as the team has experience with the textbook.

[23] A. Mardston, “Sim Vascular,” *Sim Vascular Docs*, 2024. <https://simvascular.github.io/documentation/quickguide.html> (accessed Oct. 20, 2024).

This source comes from the Sim Vascular’s github page that describes the process for setting up problems for the computational fluid dynamics solver. Detailing common issues, user guides, and

more. Providing a useful tool for modeling the team's geometries in an idealized space.

[24] M. Murakami, F. Jiang, N. Kageyama, and X. Chen, "Computational Fluid Dynamics Analysis of Blood Flow Changes during the Growth of Saccular Abdominal Aortic Aneurysm," *Annals of Vascular Diseases*, vol. 15, no. 4, pp. 260–267, Dec. 2022, doi: <https://doi.org/10.3400/avd.oa.22-00098>.

This study is crucial for a report on modeling aneurysm rupture as it offers valuable insights into the hemodynamic changes that occur during the growth of a saccular abdominal aortic aneurysm. The computational fluid dynamics (CFD) analysis in this research highlights how parameters like wall shear stress, mean flow velocity, mean pressure, energy loss, and pressure loss coefficient evolve with increasing aneurysm size.

[25] J. Xiang *et al.*, "Initial Clinical Experience with AView—A Clinical Computational Platform for Intracranial Aneurysm Morphology, Hemodynamics, and Treatment Management," *World Neurosurgery*, vol. 108, pp. 534–542, Dec. 2017, doi: <https://doi.org/10.1016/j.wneu.2017.09.030>.

This source provides a good competitor to put into the QFD. It demonstrates a model software that can predict rupture risk in intracranial aneurysms. The findings suggest that AView can support clinicians in confirming treatment decisions, prioritizing aneurysms with higher rupture risk, and improving treatment planning by providing advanced flow visualization. The study underscores the potential of AView to enhance decision-making and patient outcomes in IA management while emphasizing its ability to integrate complex data into clinical workflows. AView is tough to compare to the model-based approach found within this report, however the goals of each approach are the same.

3.2.3 Amanda Ortiz-Velazquez

[26] Á. Ugron, "Flow Simulation in Intracranial Aneurysms," ProQuest Dissertations & Theses, 2015.

This dissertation discusses the use of flow simulation to comprehend the hemodynamics involved in brain aneurysms and their ruptures. The author examines how different flow-modeling techniques can be utilized to better understand aneurysms and help improve patient-specific diagnoses and outcomes. The team chose this article because the ultimate goal of their project is to make patient-specific models that can be used to fix aneurysms. Ways of modeling flow would be incredibly useful when creating the patient-specific aneurysms models.

[27] D. M. Sforza, C. M. Putman, and J. R. Cebral, "Computational fluid dynamics in brain aneurysms," *International journal for numerical methods in biomedical engineering*, vol. 28, no. 6–7, pp. 801–808, 2012, doi: 10.1002/cnm.1481.

This paper focuses on the use of computational fluid dynamics to study how blood flow and wall geometry contribute to the formation and ultimately the rupture of brain aneurysms. This source was used because the team's current project aims to do a similar thing. However, unlike in the dissertation which is mostly mathematical model based, this project will be heavily based on experimentation. However, the use of computational fluid dynamics might prove to be useful when the team enters the replication phase of the project.

[28] P.-C. Chen et al., “Engineering additive manufacturing and molding techniques to create lifelike willis’ circle simulators with aneurysms for training neurosurgeons,” *Polymers*, <https://www.ncbi.nlm.nih.gov/pmc/articles/PMC7761873/> (accessed Sep. 9, 2024).

This source explores the use of 3D printing to create a life-like model of the willis circle. The author discusses how the properties of certain filaments can actually do a very good job in replicating the properties of brain tissue. Ideally this method could be utilized in training future neurosurgeons and perfecting or inventing new techniques for brain surgery. The team considered this article important while choosing which materials to create their own models out of.

[29] ochxlkwiz, “electric circuits 11th edition nilsson pdf.” Zenodo, Jun. 10, 2024, doi: 10.5281/ZENODO.12364277.

This book provides a detailed explanation of basic electrical circuits and components. The team utilized this source to do some preliminary calculations concerning the pump that will be used later in the project.

[30] H. E. A. Baieth, “Physical parameters of blood as a non - newtonian fluid,” *International journal of biomedical science : IJBS*, <https://www.ncbi.nlm.nih.gov/pmc/articles/PMC3614720/> (accessed Sep. 9, 2024).

This article explains the properties of blood and how it acts as a non-newtonian fluid. The paper highlights how shear rate and viscosity affect the behavior of blood in the circulatory system and therefore, are extremely important in flow simulations and analysis. The article also emphasizes that understanding the physical properties of blood is crucial in making medical devices that are compatible in the body and effective. The team looked at this article because understanding the properties of blood will be useful when ensuring that their simulation is as realistic as possible.

[31] “Blood flow - CFD simulation CFD software tutorial,” *Blood Flow CFD Simulation Software*, <https://help.sim-flow.com/tutorials/blood-flow> (accessed Sep. 16, 2024).

The above source is software available that allows for computational fluid dynamics simulation as well as provides a tutorial on how to do so. This source is important because it allows the team to test out different aneurysm types and get an idea of how they will rupture without having to create actual models which are time consuming and expensive.

[32] M. R. Harreld, “Brain aneurysm blood flow: Modeling, simulation, VR visualization,” *ProQuest Dissertations & Theses*

This source analyzes the use of virtual reality to better understand the behavior of cranial aneurysms and their ruptures. The author hopes to use VR alongside other advanced modeling techniques in order to improve risk assessments for patients as well as create better ways to map out surgery or other treatment plans. This source was useful for the team to understand brain aneurysms better.

[33] C. K. McGarry et al., “Tissue mimicking materials for imaging and therapy phantoms: A Review,” *Physics in Medicine & Biology*, Sep. 2020. doi:10.1088/1361-6560/abbd17

This was one of the many sources utilized by the team in order to find a material that could accurately mimic the mechanical properties of brain tissue. The source above showed various different tables that had information on materials that could be used to mimic different body parts. From this source we discovered that both agar and agarose have similar properties to the brain in terms of elasticity, diffusivity and density. This source helped us narrow down the possible materials we could use to make an accurate representation of the human brain.

[34] Jingyu Wang et al., “Hydrogels with brain tissue-like mechanical properties in complex environments,” *Materials & Design*, <https://www.sciencedirect.com/science/article/pii/S0264127523007530#:~:text=Several%20different%20types%20of%20hydrogels,mechanical%20behavior%20of%20brain%20tissues.> (accessed Nov. 20 2024).

The source above describes in detail how different types of gels and the brain share properties. It was due to this article that the team decided to use agarose instead of agar. While agar would be able to do a decent job in mimicking the brain tissue, agarose keeps a more similar PH level to the brain and is more heat resistant than agar.

[35] L. M. Vidal-Flores et al., “Fabrication and characterization of brain tissue phantoms using agarose gels for Ultrasound Vision Systems,” *MDPI*, <https://www.mdpi.com/2310-2861/10/8/540> (accessed Nov. 30, 2024).

This source detailed experiments using different concentrations of agarose and buffers to try and find the most realistic variation. While each of the variations of concentrations worked some worked for some things better than others. For example, a concentration of 0.7% had a similar density to the brain but it was not resistant to high heat. Whereas the concentration of 1% was firmer but it was more resistant to heat. Given that our brain tissue mimic will be suspended in a water tank with a temperature of 37 degrees Celsius, our team decided that having a solid gelatin mix at that temperature was more important than some other criteria. This source helped the team decide what range of concentrations for the agarose will be better suited for the project and demonstrated how to prepare the agarose powder for testing.

3.3 Mathematical Modeling

3.3.1 Velocity Flow Distribution in Ansys CFX - Caden

The first engineering calculation completed for this section was finding velocity distribution profiles using Ansys CFX. This calculation was performed to locate points of concern for the models, as they will need to be manually weakened to simulate a real rupture scenario. Finding the optimal places for these points of concern to apply chemicals to weaken the walls is essential for maintaining realism in this simulation. Conditions for calculation of mean flow velocity were as follows. The blood vessel and aneurysm wall surfaces were treated as no-slip rigid walls. The flow was a steady-state flow of an incompressible Newtonian fluid with a density of 1.05 g/cm^3 , and a dynamic viscosity of 0.0045 Pa s . A pressure difference to maintain a Reynolds number of approximately 400 was applied. This inflow pressure was equated to be 7.981 Pa . Calculated from the Reynolds number formula $Re = \frac{\rho * u * D}{\mu}$ [22]

where $Re = 400$, $\rho = \frac{1050 \text{ kg}}{\text{m}^3}$, $\mu = 0.0045 \text{ Pa s}$, $D = 0.01 \text{ m}$. This resulted in an average velocity (u) of 0.1714 m/s . Plugging this into the Hagen-Poiseuille Equation $\Delta P = \frac{32 * \mu * u * L}{D^2}$ [22], resulting in a pressure difference (ΔP) of 7.918 Pa , rounded to 8 Pa for analysis simplicity. These values were used for

evaluation of both models.

Table 1 Analysis conditions

Software	ANSYS CFX
Inflow Conditions	8 [Pa]
Outflow Conditions	0 [Pa]
Density of Newtonian fluid	1.05 [g/cm ³]
Viscosity of Newtonian fluid	0.0045 [Pa s]

Plugging in these parameters gives the following velocity profiles:

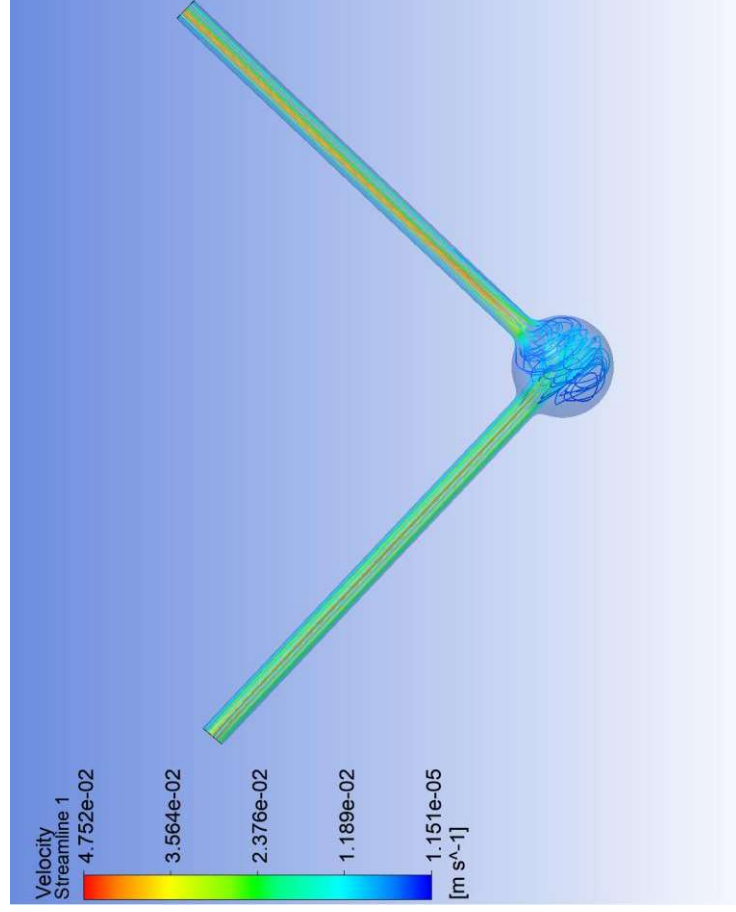


Figure 5: Flow Velocity Profile Idealized Model

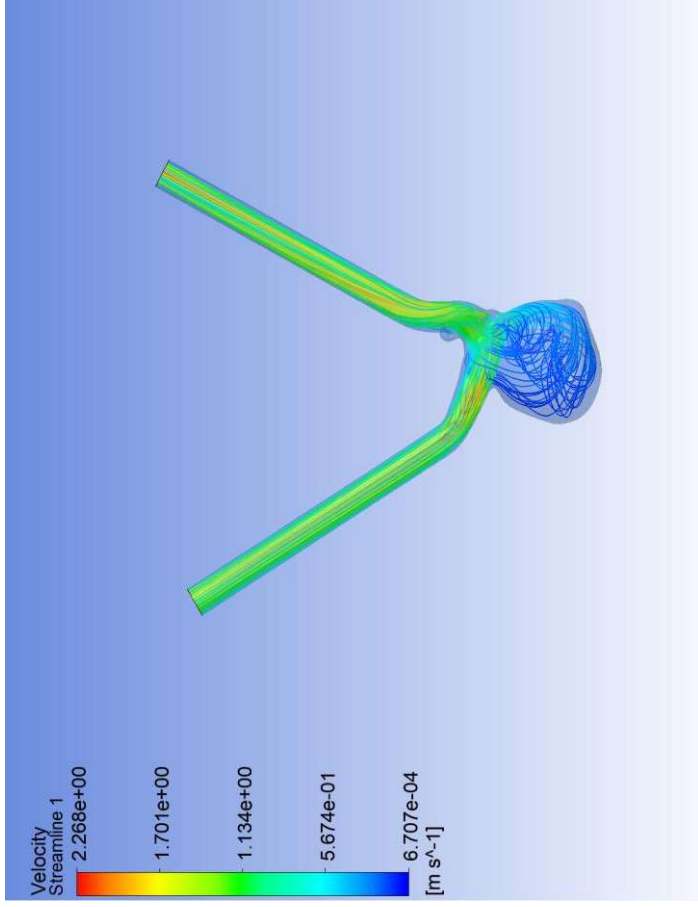


Figure 6: Flow Velocity Profile Patient Specific Model

Noticeable decreases in velocity can be seen in the head of the aneurysm in which flow drops to around 1.151×10^{-5} and 6.707×10^{-4} m/s for the idealized and patient specific vessels respectively. This also shows that the point of concern for the idealized aneurysm is almost directly across from the inlet leg, and the point of concern for the patient specific model appears to be slightly below the outlet leg.

3.3.2 Flow Characterization - Anna Mellin

In the first presentation, the Navier-Stokes equation shown in Equation 4 describes fluid movement which can be used to help characterize the flow in the model artery and compare its behavior to that of a real-life aneurysm [3].

$$\rho \left[\frac{\partial u}{\partial t} + \frac{\partial u}{\partial x} u + \frac{\partial u}{\partial y} v + \frac{\partial u}{\partial z} w \right] = -\frac{\partial p}{\partial x} + \mu \left(\frac{\partial^2 u}{\partial x^2} + \frac{\partial^2 u}{\partial y^2} + \frac{\partial^2 u}{\partial z^2} \right) + \rho g_x$$

(Equation 4: Navier-Stokes)

Another equation to characterize the model is Laplace's Law (Equation 5), which describes the tension in the wall of the aneurysm [1].

$$T = \frac{PR}{2} \quad (\text{Equation 5: Laplace's Law})$$

T = tension

P = internal pressure

R = radius

If P = 12443.3784 Pa (using Equation 6), and R = 0.010 m for a large aneurysm, the tension is

$$T = \frac{12443.3784 \text{ Pa} * 0.010 \text{ m}}{2} = 124.43 \text{ Pa} * m \text{ (Equation 6)}$$

Which if compared with the tension the aneurysm wall can withstand, will tell us if the aneurysm will burst or not.

The next equation, also based on Laplace's Law, demonstrates the stress within the wall of the aneurysm.

$$\sigma = \frac{Pr}{2W}$$

The variables in these equations represent the following:

σ = wall stress

P = Internal Pressure

r = radius

2 = wall thickness

$$\sigma = \frac{12443.3784 \text{ Pa} * 0.01 \text{ m}}{2 * 0.75 \text{ m}} = 165.91 \text{ Pa}$$

This equation will help dictate where the aneurysm is most likely to burst (by examining wall thickness) and again, whether the silicone will be able to withstand the stress inflicted upon it.

3.3.3 Estimating Time for Resin to Dissolve - Amanda Ortiz-Velazquez

The last calculation performed was the Noyes-Whitney Equation shown below. This equation provides an estimation for how long it will take for the water-soluble resin to completely dissolve in water.

$$dM/dt = (DA(C_s - C))/L \text{ (Equation 7: Noyes-Whitney)}$$

The variables in these equations represent the following:

DM/dt = rate of mass dissolved per unit time
D = diffusion coefficient

A = Surface area

C_s = saturation concentration

C = concentration of solute in solvent at time
L = thickness of boundary layer

In order to conduct the calculations using this equation, a few assumptions were made. Diffusion coefficient and saturation concentration are not listed for the exact type of resin that we will be using so the team had to take the average numbers for these factors for other available water-soluble resins.

$$dM/dt = ((1 \times 10^{-5}) \text{cm}^2) \times (5.52 \text{ cm}^2) \times (0.5 \text{ g/L}) / 0.01 \text{ cm} = 2.76 \times 10^{-3} \text{ g/s}$$

With 6 grams of resin and a surface area of 5.52 cm²:

$$(6 \text{ g}) / (2.76 \times 10^{-3} \text{ g/s}) = 2174 \text{ seconds}$$

$$2174 \text{ seconds} = 36.2 \text{ minutes}$$

According to the calculations, it would take about 36 minutes for the water-soluble resin to completely dissolve with room temperature water (78 degrees Fahrenheit) and no agitation.

4 Design Concepts

4.1 Functional and Physical Decomposition

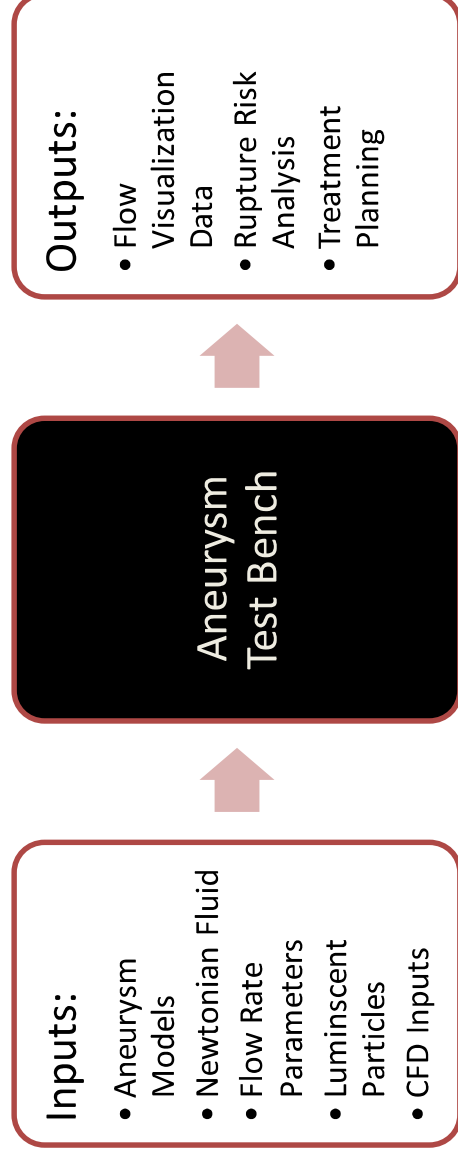


Figure 7: Functional Decomposition (Black Box Model)

Pictured above is the functional decomposition for this project, starting with the end goal of a mobile operating aneurysm test bench. This decomposition is important to the project as the client needs and mentor instructions are not as finite or linear as other projects. A lot of this work is up to interpretation, so having a model that lays out the required inputs and outputs, which are key to the success of the project.

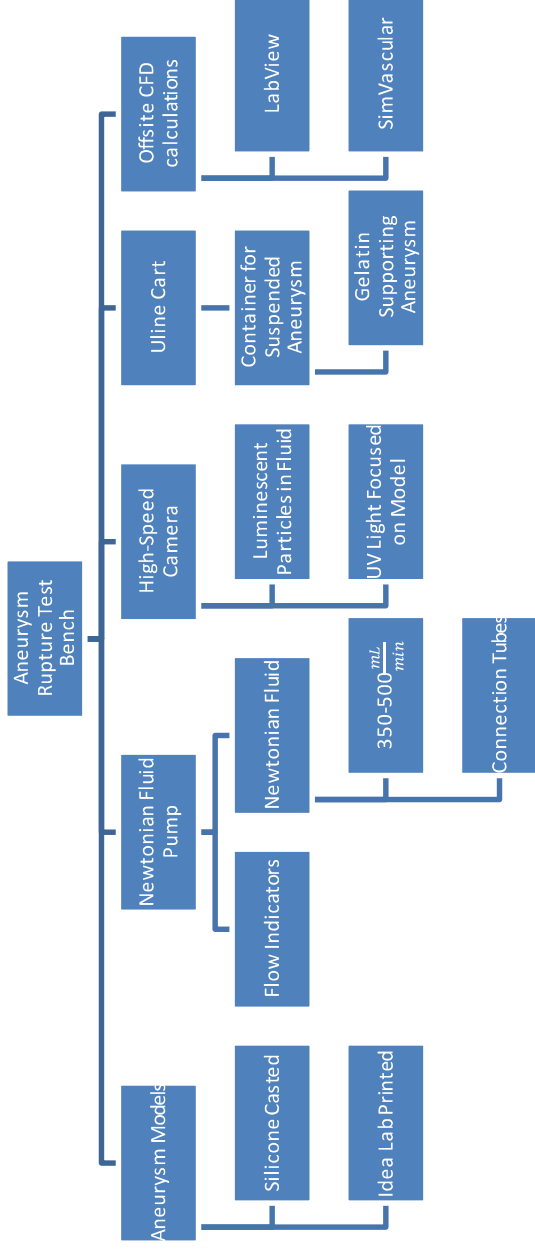


Figure 8: Physical Decomposition

This decomposition breaks down the complex tasks of the project into manageable subtasks, in which all aspects of the project are accounted for, guiding the direction of the project with the overarching goal of creating a realistic simulation environment for aneurysm treatment procedures.

4.2 Concept Generation

4.2.1 Support System

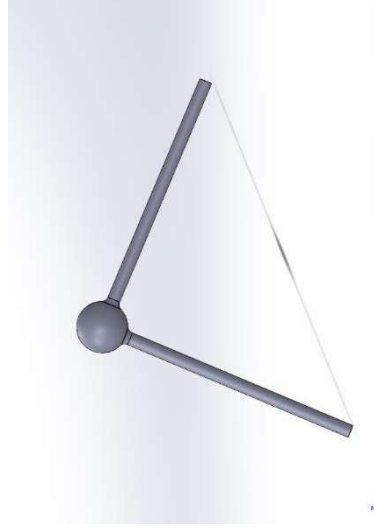


Figure 9: No Support System

Figure 9 above depicts the original design which has no supports. This design was not chosen because it did not meet the necessary requirements. Without supports, the structure would move once the silicone was inserted and the walls of the model would not be uniform. However, this design was the easiest to create and did have the lowest production cost.



Figure 10: Cylindrical Support System

The second design shown in the figure above had two cylindrical supports on either end of the structure. While this design did use less material than some of the other designs, it would not provide adequate support, and silicone would leak out of mold through the ends.



Figure 11: Cylindrical Supports along structure

This above design shows cylindrical supports along the structure on one side. This design provided the most support as every area of the structure had a support. However, not only did this design use the most amount of material which made it difficult to design and would increase manufacturing cost, it would also create issues in the postproduction of the model. When the mold would be filled with silicone, the silicone would harden around these cylinders creating holes in the structure. It would then be necessary to find a way to cover these holes after the model hardened and ensure that the patches were even. Due to this, the design shown in the figure above was chosen as it did not meet the requirements for the project.

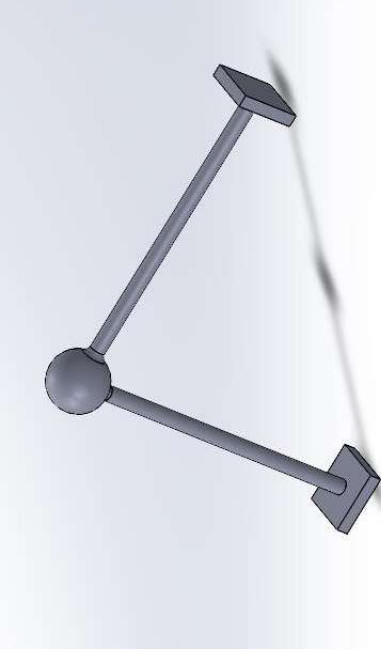


Figure 12: Square Supports

Figure 12 shows the final design with square supports on both ends of the structure. This design would provide the needed support without compromising the structure. The square ends would slot into holes in the mold which would keep the silicone from leaking out of the sides. Despite having a slightly higher production cost than some of the other designs, this design was chosen as it would be the simplest while still satisfying the other criteria.

4.2.2 Negative Molds

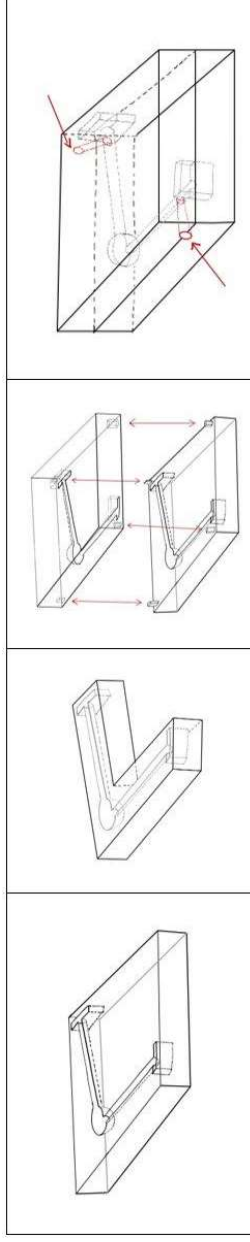


Figure 13: Negative mold concepts, from left to right: Idea 1: basic square negative, Idea 2: negative without excess, Idea 3: with keys, male and female parts, Idea 4: with holes for silicone injection.

Idea 1 was the generic concept. It fulfilled the basic requirements of creating a cavity with a space of 0.75 mm for wall thickness while keeping the silicone in place. Idea 2 was formulated as a means of reducing cost. By removing unnecessary material, the expenses are reduced. Idea 3 was developed as a potential means of reducing error. By creating keys with male and female parts for the two sides of the negative mold to fit together, the parts will not be able to slide around and there is less of a risk of deformity. Idea 4 was produced to increase accuracy of the anatomical model. By injecting silicone through holes, the parts are again less likely to slide (as they will be adhered to each other before injection) and deformity is again less likely to occur.

4.2.3 Negative Mold Conception

When producing the hollow models, there was not much leeway in terms of development. The various

methods included SolidWorks attempts with various methods of hollowing out the complex geometries, but this failed multiple times as the files used primarily were mesh STL files, which SolidWorks has a very difficult time working with. After these trials and errors, the focus was shifted to Meshmixer, in which the body could be hollowed out with specified parameters providing a much simpler way to model. Meshmixer was also a crucial tool for smoothing and changing the size of the models as it was designed to work with the mesh bodies used in this project. The team plans to use more SolidWorks in the mold generation previously stated.

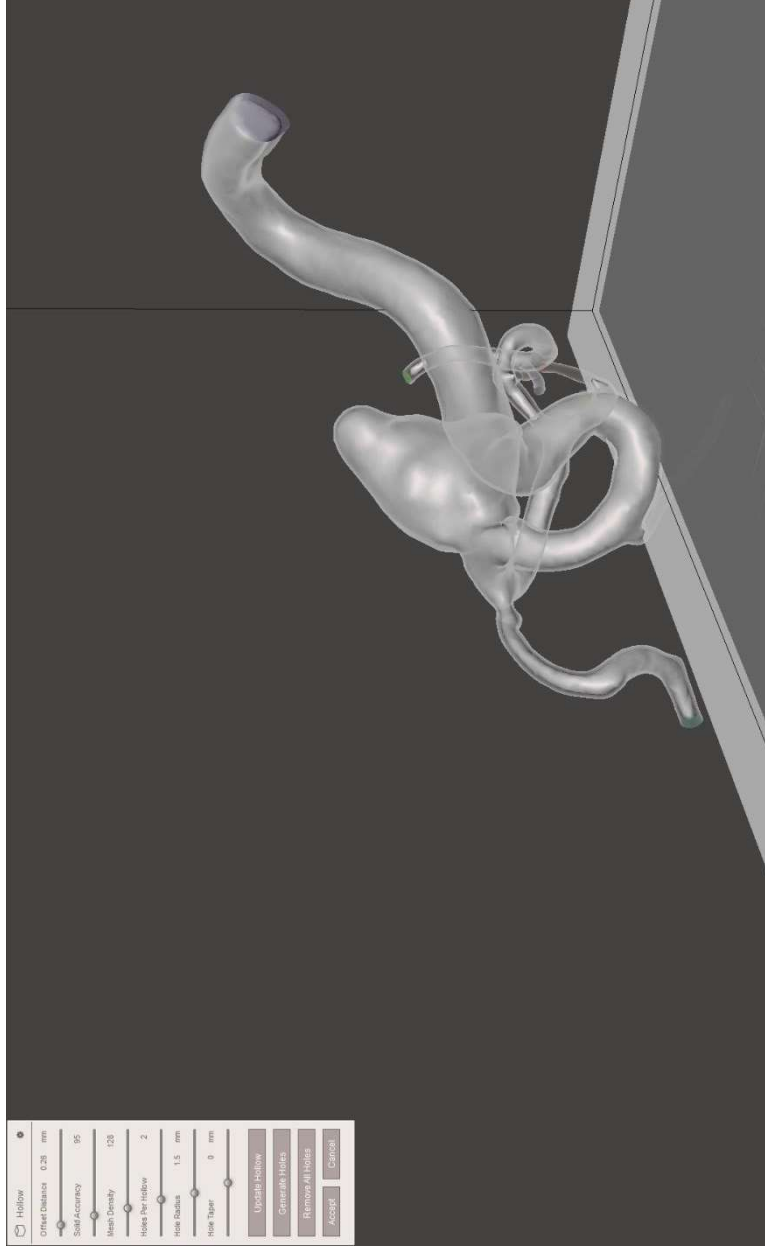


Figure 14: Meshmixer Hollow Feature

4.3 Selection Criteria

After meeting with the client, Dr. Zhongwang Dou, a list of criteria was provided which entailed the concepts that the project must meet. Additional requirements were also added as the project progressed. These customer requirements and criteria included cost, simplicity, user-friendliness, reusability, precision, and effectiveness. The material being used for the resin printer costs approximately \$50 per bottle, due to this, the team decided that the concepts that utilized the least amount of material would be preferred. For precision the team needed the dimensional accuracy to be within 0.15 mm. For the final design the product must be within 0.10mm. The reusability aspect refers mainly to how easy the design is to reprint; this came down to how big the design was and how many fragile parts were included in each concept. This requirement is almost directly correlated to the cost. The smaller the part, the easier it is to print and the lower the cost. User-friendliness is measured by how much time it took to create the design and how much time it will take to make the silicone model. Effectiveness depends on how well the blood-like fluid is able to flow through the material. Lastly, simplicity will be measured by how much time it takes from the moment the design begins printing to when the hollow silicone model is finished.

4.4 Concept Selection

The team created two Pugh charts as shown below, in order to analyze which concept would best satisfy the requirements. The first Pugh chart shown in figure 12 was created for the selection of the support type for the solid model. In this chart the design with no support was chosen to be the reference as it was the most straightforward of the design choices. As can be seen below in figure 12, the square supports were best. The cylinder support along the structure was not chosen because it would have been too costly and was not effective nor simple. The team also decided against the other cylinder support system because while it was not necessarily a bad design, it did not have more advantages than the square supports.

Criteria	Weight	No supports	Cylinder Support	Cylinder supports along structure	Square supports
Cost	4	0	-	--	-
Simplicity	2	0	-	--	-
User Friendly	3	0	0	-	0
Reusability	5	0	0	0	0
Precision	5	0	0	--	++
Effectiveness	5	0	0	-	++
Plus			0	0	2
Minus			2	5	2
Zero			5	2	2
			-2	-5	0

Figure 15: Positive Solid Models Pugh Chart

For the concept selection of the negative mold, a Pugh chart, shown in Figure 13 was created to demonstrate how the concepts compared to Idea 1, the base design. Idea 1 was chosen to be the reference as it was the simplest of the models.

Criteria	Weight	Basic Square	Excess removed	Silicone injection holes
Cost	4	0	++	+
Simplicity	2	0	+	-
User Friendly	3	0	0	-
Reusability	5	0	0	0
Precision	5	0	0	0
Effectiveness	5	0	0	0
Plus			2	1
Minus			0	2
Zero			4	3
			2	-1

Figure 16: Negative mold Pugh chart

According to the chart, Idea 2 was the best. Idea 1 was eliminated simply because it added nothing that

Idea 2 cannot produce, and it is more costly. Idea 3 was eliminated because it was assumed that it may create complications with silicone removal. Plus, high levels of printing accuracy are required to ensure that not only are the cavities printing correctly but that the keys fit smoothly and snugly together as well. Essentially it was a lot of unnecessary labor that may have become a complex issue in the future.

5 Schedule and Budget

5.1 Schedule

Figure 16 shows the main milestones for the project. Appendix B shows the full Gantt Chart.

1	Hardware Model	Mon 8/26/24	Thu 12/12/24	109	86%	79
1.1	Develop Casting model	Wed 9/11/24	Sun 11/10/24	35	100%	43
1.1.1	Obtain Core Models	Wed 9/11/24	Wed 9/18/24	7	100%	6
1.1.2	Add supports to models	Thu 9/19/24	Tue 9/24/24	5	100%	4
1.1.3	Create model negatives	Thu 9/19/24	Tue 9/24/24	5	100%	4
1.2	Create Silicone Casting model	Mon 11/04/24	Wed 11/13/24	59	50%	8
1.3	Perfect Casting model and rapid produce	Mon 11/11/24	Wed 1/08/25	59	0%	43
1.4	Learn Resin Printer	Fri 9/13/24	Fri 9/13/24	1	100%	1
1.5	Preview Becker's Model	Mon 9/16/24	Mon 9/16/24	1	100%	1
1.6	Develop 3D Printed model	Thu 9/26/24	Tue 10/15/24	20	100%	14
1.5.1	Create Hollow Model	Thu 9/19/24	Tue 9/24/24	5	100%	4
1.6	Perfect 3D Printed model	Tue 10/15/24	Thu 12/12/24	59	75%	43
1.7	Design Aneurysm holder	Wed 10/30/24	Thu 11/07/24	59	95%	7
1.8	Research Brain tissue mimic	Wed 10/30/24	Thu 11/07/24	59	80%	7
1.9	Research Blood mimic	Wed 10/30/24	Thu 11/07/24	59	100%	7

Figure 17: Gantt Chart

5.2 Budget

Donation:	From Who	Amount
Machines		
Mars 4 3D Printer	Dr. Dou's Lab	\$ 271.25
Anycubic Photon M3 Printer	Dr. Dou's Lab	\$ 179.00
Mercury Plus 2 in 1	Dr. Dou's Lab	\$ 79.99
Pump	Dr. Dou's Lab	\$ 500.00
Transonic Flowmeter	Dr. Dou's Lab	\$ 112.00
Stethoscope	Dr. Dou's Lab	\$ 24.95
Plastic Tubing	Dr. Dou's Lab	\$ 10.99
Plastic Clamps	Dr. Dou's Lab	\$ 8.29
Spin-lock Stopcock	Dr. Dou's Lab	\$ 3.81
Highspeed Camera	Dr. Dou's Lab	\$1,500.00
National Instruments DAQ	Dr. Dou's Lab	\$ 245.00
Material		
Anycubic ABS-Like Resin	Dr. Dou's Lab	\$ 29.69
Elegoo 3.0 ABS-Like Resin	Dr. Dou's Lab	\$ 31.18
Sylgard Silicone Elastomer	Dr. Dou's Lab	\$ 179.90
Lab grade Gelatine	Dr. Dou's Lab	\$ 59.00
Water Soluble Resin	Dr. Dou's Lab	\$ 27.99
Acrylic Sheets	Dr. Dou's Lab	\$ 3.49
JB Weld Plastic Bonder	Dr. Dou's Lab	\$ 6.98
Gorilla Glue	Dr. Dou's Lab	\$ 12.30

Figure 18: List of materials and their commercial expenses.

Budget:	\$	1,000.00
Fundraising needed:	\$	100.00
Fundraising Obtained	\$	3,233.35
Spent:	\$	74.50
Leftover	\$	925.50

Figure 19: Budget

The starting budget is \$1000 with a required 10% of the budget fundraised (\$100). Figure 18 shows the list of materials and machinery used with their commercial costs had they not been donated by Dr. Dou's lab. Figure 19 shows the true budget and the current expenditures of the Aneurysm rupture team.

5.3 Bill of Materials

Figure 20 is the list of materials and their costs for the 3D printed model, the silicone model, the brain mimic, and the box to hold the silicone model.

Spent:	Quantity	Cost per unit	Total
Idea Lab prints	2	\$ 30.00	\$ 60.00
Negative Mold	200g	\$ 0.03	\$ 6.24
Silicone	.5 oz	\$ 10.22	\$ 5.11
Silicone Model Total			\$ 11.35
Panels	1 sheet	\$ 0.87	\$ 0.87
JB Weld Plastic Bonder	5 mL	\$ 0.28	\$ 1.40
Gorilla Glue	.25 oz	\$ 1.54	\$ 0.39
Box Total			\$ 2.65
Brain mimic	4.2 g	\$ 0.12	\$ 0.50
			\$ 74.50

Figure 20: Bill of Materials

6 Design Validation and Initial Prototype

6.1 Failure Modes and Effects Analysis (FMEA)

The Failure Modes and Effects Analysis was developed in Figure 21 to predict possible failures in the project so that they may be corrected before they occur or cause damage. Most of the predicted errors were quite severe, however, they are also not very likely to occur due to their nature of either just being extremely unlikely or because the process of manufacturing would catch them before they would occur.

Part # and Functions	Part Name	Potential Failure Mode	Potential Effect(s) of Failure	Severity (S)	Potential Causes and Mechanisms of Failure	Occurrence (O)	Current Design Controls/ Test	Detection (D)	RPN	Recommended Action
1	Cart	Structural failure	Disassembly of the entire assembly	6	Assembly error	2	Check stability	1	12	Reassembly cart
2	Hot water bath container	Structural failure	Leaks which would lower flow rate	6	Wear Sudden force	2	Check for leaks when filled with fluid	1	12	Patch leaks or use another tub
3	Pump	Flow rate deviation Motor failure	Flow doesn't match with human body function. Pump shuts down	8	Pump wear Blockage	4	Check with concomitant method	2	64	Check pump settings Clean pump
4	Hot water bath temperature regulator	Inadequate heating	Inaccurate flow model	7	Ineffective heating element Wear	4	Check temperature with a thermometer	2	56	Either recalibrate or find error and set with that accounted for
5	Flow Sensors	Calibration issues	Inaccurate readings	8	Mechanical wear Particle contamination	5	Check with concomitant method	2	80	Ensure sensors are clean and calibrated
6	Aneurysm model holder	Structural failure	Doesn't hold aneurysm securely	8	Inproper dimensions	5	Check dimensions and fit	1	40	Redesign
7a	Patient Specific Positive Cast	Deviation from Intended Geometry	Doesn't fit in negative cast! Uneven wall thickness	10	Bad print settings Wrong geometry in solidworks	5	Check the fit of the cast	1	50	Reprint
7b	Ideal Positive Cast	Deviation from Intended Geometry	Doesn't fit in negative cast! Uneven wall thickness	10	Bad print settings Wrong geometry in solidworks	5	Check the fit of the cast	1	50	Reprint
8a	Patient Specific Negative Cast A	Deviation from Intended Geometry	Doesn't fit in negative cast! Uneven wall thickness	10	Bad print settings Wrong geometry in solidworks	5	Check the fit of the cast	1	50	Reprint
8b	Patient Specific Negative Cast B	Deviation from Intended Geometry	Doesn't fit in negative cast! Uneven wall thickness	10	Bad print settings Wrong geometry in solidworks	5	Check the fit of the cast	1	50	Reprint
8c	Ideal Negative Cast A	Deviation from Intended Geometry	Doesn't fit in negative cast! Uneven wall thickness	10	Bad print settings Wrong geometry in solidworks	5	Check the fit of the cast	1	50	Reprint
8d	Ideal Negative Cast B	Deviation from Intended Geometry	Doesn't fit in negative cast! Uneven wall thickness	10	Bad print settings Wrong geometry in solidworks	5	Check the fit of the cast	1	50	Reprint
9	Tubing	Seal failure	Leaks which would lower flow rate	8	Poor fitting Wear and tear	4	Check for leaks when running	1	32	Use another tube or seal
10	Blood Mimic	Inadequate representation	Inaccurate flow model	9	Wrong composition	4	Test fluid properties to make sure they match blood properties	1	36	Research blood mimics well Conduct numerous property tests
11	High Speed Camera	Calibration issues	Inaccurate readings	8	Lens misalignment Lighting conditions	5	Check if readings make sense	2	80	Ensure camera is on stable mounting Ensure lens is clean Ensure lighting is sufficient

Figure 21: Failure Modes and Effects Analysis

6.2 Initial Prototype

The first prototype is of the patient-specific model suspended in water, which serves to test if the models produced can withstand the pressure and velocity of fluid present in the testing bench. This also acts primarily to test if the setup used is sufficient to extract data into LabVIEW. After attaching the models to the pump system, the team found that the aneurysms are of appropriate thickness which allows for sufficient fluid flow and resist preemptive rupture. It was also noted that the test bench is well set up and allows for efficient and effective data collection. Moving forward, we know that this exact print may be used, with the only adjustment being the thinning of a spot to produce a weak point that will allow for rupture. While effective, the pump system still requires model holders and stabilizers.

The second prototype was the model suspended in G6650 gelatin to see if this material sufficiently mimicked the brain. We found that the gelatin produced a yellow tint which is not ideal for observation, and did not harden to the desired specifications. Moving forward, a higher ratio of gelatin will be tested

alongside other materials such as agarose.

The third prototype was a flow simulator using SolidWorks. This showed the general area where a weak spot might form. Although it gave us a relative location, ANSYS provided a more exact and reliable area to weaken.

6.3 Additional Engineering Calculations

An uncertainty analysis was implemented to find the main source of error when calculating the flowrate in the pump system.

The flowrate equation is given by Equation A:

$$Q = SPM * V \text{ (Equation A)}$$

$$Q = \text{Flowrate}$$

$$SPM = \text{Strokes per minute}$$

$$V = \text{Volume}$$

The zero-order uncertainty of the instrument is given by Equation B:

$$u_0 = \frac{1}{2} * \text{resolution} = 1 \text{ LSD (Equation B)}$$

LSD = Lowest significant Digit

Equation C is the error propagation and allows uncertainties to be put into the same units (mL/min).

$$u_Q = \frac{\partial Q}{\partial SPM} u_{SPM} \text{ (Equation C.1)}$$

$$u_Q = \frac{\partial Q}{\partial V} u_V \text{ (Equation C.2)}$$

Equation D is the root mean sum of squares and is used to find the total uncertainty:

$$u_T = \sqrt{u_1^2 + u_2^2 + \dots + u_n^2} \text{ (Equation D)}$$

The uncertainties of the flowmeter and the pump were analyzed with the previous equations:

$$u_{SPM} = \frac{1}{2} \cdot 20 \frac{\text{strokes}}{\text{min}} = 10 \frac{\text{strokes}}{\text{min}}$$

$$u_V = \frac{1}{2} \cdot 1 \text{ mL} = 0.5 \text{ mL}$$

Taking the pump at 2.5 mL at 60 strokes/min:

$$u_Q = 60 \frac{\text{strokes}}{\text{min}} \cdot 0.5 \text{ mL} = 30 \frac{\text{mL}}{\text{min}}$$

$$u_Q = 2.5 \frac{\text{mL}}{\text{min}} \cdot 10 \frac{\text{strokes}}{\text{min}} = 25 \frac{\text{mL}}{\text{min}}$$

$$u_{\text{flowmeter}} = 5 \frac{\text{mL}}{\text{min}}$$

Using the root mean sum of squares to find the total uncertainty:

$$u_T = \sqrt{25^2 + 30^2 + 5^2} = 39.37 \frac{mL}{min}$$

Which shows that the major source of error comes from the pump and not the flow sensor, which is to be expected.

6.4 Future Testing Potential

So far, this document has demonstrated the technical details of the project but has failed to take any of the information off the page. For this section the equipment used, resources, space, and testing procedures will all be addressed.

First, the equipment used at the top level consists of a Lauda ECO Gold hot water bath heated to 37°C to mimic conditions found in the human body in which the vessel will be held in. A water pump drives the pressure and velocity of Newtonian fluid flow into the vessel. This is connected to a flow controller designed to mimic pulsatile cardiac flow. This flows into a pressure transducer on the inlet and through the aneurysm into another transducer on the outlet tube. These pressure transducers are connected to a laptop running LabView via a USB controller. Parts not listed such as the vessel holder, and model casts were printed using Anycubic photon M3 and the Elegoo Mars 4 resin printers. These are cured in an Anycubic Mercury two in one. The data is captured visually for comparison against recorded data with a high-speed camera.

Resources for this project include resin, the equipment listed above, clear acrylic sheets, several varieties of glue, gelatin from bovine skin, 99% isopropyl alcohol, and a Newtonian blood mimic consisting of glycerin, salt, and water. The resin used is Elegoo ABS-like Resin V3.0, Anycubic ABS-like plant-based resin, and Anycubic water-wash resin.

The space required for this project is designed to be non-obstructive and mobile. The entire setup is contained on a two-level U-line cart. All testing will be conducted on the cart. Printing and other miscellaneous part construction is done in the Bio propulsion Lab headed by Dr. Dou.

The testing procedure is as follows:

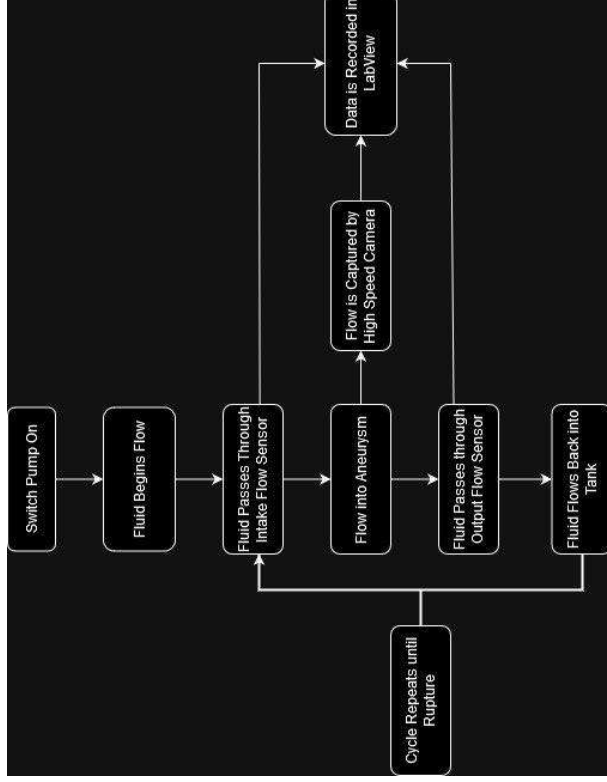


Figure 22: Testing Procedure

Data is all synced and collected in LabView, and the system runs in a closed loop so it is able to effectively run infinitely until a rupture is observed. Ideally, rupture will occur within 5 minutes of turning on the pump, this result will be achieved through iteration over the course of next semester.

7 CONCLUSIONS

Dr. Zhongwang Dou assigned our team with a project to find an effective way of recreating an aneurysm rupture simulation that could be adjusted for patient-specific cases. This model would be connected to a pump and suspended in gelatin with a blood-like fluid pumping through it in order to create the most realistic conditions. This project must be effective, predictable, and measurable.

The report above describes in detail the design process as well as the final concept. Section one discusses the goals and direction for the aneurysm rupture project. The model will be made with both 3D printing and wax casting techniques which will both be tested to discover which one yields better results. The model will need to replicate the real-life phenomena of an aneurysm rupturing. This will be recorded using a high-speed camera as well as flow and pressure sensors. The next section of the document describes the requirements which were given to the team by the client. These requirements include but are not limited to repeatability, consistency, and effectiveness. To gauge a good starting point, the team did research on existing models which were similar as a way to get a benchmark. These benchmarks are the Kono Aneurysm model, Sigiu model, and the Lui model which are all further detailed in section three. The team then continued to do more research and compiled a list of resources which were beneficial to the project and are summarized in section 3.2. The mathematical models are included later in the document and provide a description of which equations were used and why they are important. The next section depicts the concept generation as well as the selection process of mentioned concepts. The concepts were split into three main components. These were the hollow versions of the aneurysms, the solid versions, and the mold. Several concepts were generated and then inserted into a Pugh chart to help the team decide. In the end, the team chose to make the square supported structure and the mold that will

require the excess silicone to be removed.

In the previous weeks the team has successfully created a mold for two of the aneurysm types. They plan to begin testing with silicone and water-soluble resin within the next few weeks. Once testing begins the team hopes to have a working model that will be capable of advancing the medical devices available to prevent or fix aneurysms, thus resulting in a decreased loss of life due to aneurysm ruptures.

8 REFERENCES

- [1] “Pressure,” *hyperphysics.phy-astr.gsu.edu*. <http://hyperphysics.phy-astr.gsu.edu/hbase/ptens.html>
- [2] “Vascular Model Repository,” *Vascularmodel.com*, 2024. <https://www.vascularmodel.com/index.html> (accessed Sep. 14, 2024).
- [3] R. Fox, A. McDonald, and J. Mitchell, *Fox and McDonald's Introduction to Fluid Mechanics*, 10th ed. 111 River Street Hoboken, NJ: John Wiley & Sons, 2020.
- [4] Mayo Clinic, “Brain aneurysm - Symptoms and causes,” *Mayo Clinic*, Mar. 07, 2023. <https://www.mayoclinic.org/diseases-conditions/brain-aneurysm/symptoms-causes/syc-20361483>
- [5] Kono K, Shintani A, Okada H, Terada T. Preoperative simulations of endovascular treatment for a cerebral aneurysm using a patient-specific vascular silicone model. *Neurol Med Chir (Tokyo)*. 2013;53(5):347-51. doi: 10.2176/nmc.53.347. PMID: 23708228.
- [6] Sugiu K, Martin JB, Jean B, Gailloud P, Mandai S, Rufenacht DA. Artificial cerebral aneurysm model for medical testing, training, and research. *Neurol Med Chir (Tokyo)*. 2003 Feb;43(2):69-72; discussion 73. doi: 10.2176/nmc.43.69. PMID: 12627882.
- [7] Liu, Y. *et al.* Fabrication of cerebral aneurysm simulator with a desktop 3D printer. *Sci. Rep.* 7, 44301; doi: 10.1038/srep44301 (2017).
- [8] J. R. Ryan, K. K. Almeyty, P. Nakaji, and D. H. Frakes, “Cerebral Aneurysm Clipping Surgery Simulation Using Patient-Specific 3D Printing and Silicone Casting,” *World Neurosurgery*, vol. 88, pp. 175–181, Apr. 2016, doi: <https://doi.org/10.1016/j.wneu.2015.12.102>.
- [9] N. Hopkinson, Richard Hague, and Philip Dickens, *Rapid Manufacturing An Industrial Revolution for the Digital Age*. The Atrium, Southern Gate, Chichester, West Sussex PO19 8SQ England: John Wiley & Sons, Ltd, 2006.
- [10] “Flow Diversion with Stents for Brain Aneurysms,” Dec. 28, 2022. <https://www.hopkinsmedicine.org/health/treatment-tests-and-therapies/flow-diversion-with-stents-for-brain-aneurysms#:~:text=What%20is%20flow%20diversion%20for>
- [11] “Endovascular Coiling,” *John Hopkins Medicine*, 2019. <https://www.hopkinsmedicine.org/health/treatment-tests-and-therapies/endovascular-coiling>
- [12] “Microsurgical Clipping and Endovascular Coiling for Brain Aneurysm,” www.hopkinsmedicine.org. <https://www.hopkinsmedicine.org/health/treatment-tests-and-therapies/microsurgical-clipping-and-endovascular-coiling-for-brain-aneurysm>
- [13] R. G. Nagassa, P. G. McMenamin, J. W. Adams, M. R. Quayle, and J. V. Rosenfeld, “Advanced 3D printed model of middle cerebral artery aneurysms for neurosurgery simulation,” *3D Printing in Medicine*, vol. 5, no. 1, Aug. 2019, doi: <https://doi.org/10.1186/s41205-019-0048-9>.

- [14] M. S. Pravdivtseva *et al.*, “3D-printed, patient-specific intracranial aneurysm models: From clinical data to flow experiments with endovascular devices,” *Medical Physics*, vol. 48, no. 4, pp. 1469–1484, Feb. 2021, doi: <https://doi.org/10.1002/mp.14714>.
- [15] J. R. Cebal *et al.*, “Aneurysm Rupture Following Treatment with Flow-Diverting Stents: Computational Hemodynamics Analysis of Treatment,” *American Journal of Neuroradiology*, vol. 32, no. 1, pp. 27–33, Nov. 2010, doi: <https://doi.org/10.3174/ajnr.a2398>.
- [16] L.-D. Jou and M. E. Mawad, “Analysis of Intra-Aneurysmal Flow for Cerebral Aneurysms with Cerebral Angiography,” *American Journal of Neuroradiology*, vol. 33, no. 9, pp. 1679–1684, May 2012, doi: <https://doi.org/10.3174/ajnr.a3057>.
- [17] W. C. Merritt, H. F. Berns, A. F. Ducruet, and T. A. Becker, “Definitions of intracranial aneurysm size and morphology: A call for standardization,” *Surgical Neurology International*, vol. 12, p. 506, Oct. 2021, doi: <https://doi.org/10.25259/SNI.576.2021>.
- [18] K. W. Yong, M. Janmaleki, M. Pachenari, A. P. Mitha, A. Sanati-Nezhad, and A. Sen, “Engineering a 3D human intracranial aneurysm model using liquid-assisted injection molding and tuned hydrogels,” *Acta Biomaterialia*, vol. 136, pp. 266–278, Dec. 2021, doi: <https://doi.org/10.1016/j.actbio.2021.09.022>.
- [19] C. Patel, “Acquiring Data from Sensors and Instruments Using MATLAB.” Available: <https://www.mathworks.com/content/dam/mathworks/mathworks-dot-com/solutions/automotive/files/in-expo-2012/acquiring-data-from-sensors-and-instruments-using-matlab.pdf>
- [20] L. Bousset *et al.*, “Aneurysm Growth Occurs at Region of Low Wall Shear Stress,” *Stroke*, vol. 39, no. 11, pp. 2997–3002, Nov. 2008, doi: <https://doi.org/10.1161/strokeaha.108.521617>.
- [21] The Engineering Toolbox, “Dynamic Viscosity of common Liquids,” *Engineeringtoolbox.com*, 2019. https://www.engineeringtoolbox.com/absolute-viscosity-liquids-d_1259.html
- [22] F. M. White, *Fluid Mechanics*, 7th ed. McGraw Hill, 2011.
- [23] A. Mardston, “SimVascular,” *SimVascular Docs*, 2024. <https://simvascular.github.io/documentation/quickguide.html> (accessed Oct. 20, 2024).
- [24] M. Murakami, F. Jiang, N. Kageyama, and X. Chen, “Computational Fluid Dynamics Analysis of Blood Flow Changes during the Growth of Saccular Abdominal Aortic Aneurysm,” *Annals of Vascular Diseases*, vol. 15, no. 4, pp. 260–267, Dec. 2022, doi: <https://doi.org/10.3400/avd.oa.22-00098>.
- [25] J. Xiang *et al.*, “Initial Clinical Experience with AVIEW—A Clinical Computational Platform for Intracranial Aneurysm Morphology, Hemodynamics, and Treatment Management,” *World Neurosurgery*, vol. 108, pp. 534–542, Dec. 2017, doi: <https://doi.org/10.1016/j.wneu.2017.09.030>.
- [24] Á. Ugron, “Flow Simulation in Intracranial Aneurysms,” ProQuest Dissertations & Theses, 2015.
- [25] D. M. Sforza, C. M. Putman, and J. R. Cebal, “Computational fluid dynamics in brain aneurysms,” *International journal for numerical methods in biomedical engineering*, vol. 28, no. 6–7, pp. 801–808, 2012, doi: [10.1002/cnm.1481](https://doi.org/10.1002/cnm.1481).

- [26] P.-C. Chen et al., “Engineering additive manufacturing and molding techniques to create lifelike willis’ circle simulators with aneurysms for training neurosurgeons,” *Polymers*, <https://www.ncbi.nlm.nih.gov/pmc/articles/PMC7761873/> (accessed Sep. 9, 2024).
- [27] ochlxzwiz, “electric circuits 11th edition nilsson pdf.” Zenodo, Jun. 10, 2024, doi: 10.5281/ZENODO.12364277.
- [28] H. E. A. Baieth, “Physical parameters of blood as a non - newtonian fluid,” *International journal of biomedical science : IJBS*, <https://www.ncbi.nlm.nih.gov/pmc/articles/PMC3614720/> (accessed Sep. 9, 2024).
- [29] “Blood flow - CFD simulation CFD software tutorial,” *Blood Flow CFD Simulation Software*, <https://help.sim-flow.com/tutorials/blood-flow> (accessed Sep. 16, 2024).
- [30] M. R. Harreld, “Brain aneurysm blood flow: Modeling, simulation, VR visualization,” *ProQuest Dissertations & Theses*
- [33] C. K. McGarry et al., “Tissue mimicking materials for imaging and therapy phantoms: A Review,” *Physics in Medicine & Biology*, Sep. 2020. doi:10.1088/1361-6560/abbd17
- [34] Jingyu Wang a 1 et al., “Hydrogels with brain tissue-like mechanical properties in complex environments,” *Materials & Design*, <https://www.sciencedirect.com/science/article/pii/S0264127523007530#:~:text=Several%20different%20types%20of%20hydrogels,mechanical%20behavior%20of%20brain%20tissues.> (accessed Nov. 20 2024).
- [35] L. M. Vidal-Flores et al., “Fabrication and characterization of brain tissue phantoms using agarose gels for Ultraviolet Vision Systems,” *MDPI*, <https://www.mdpi.com/2310-2861/10/8/540> (accessed Nov. 30, 2024).

9 Appendix A: Full Gantt Chart

